Cell Research (2013) 23:444-447.

www.nature.com/cr

LETTER TO THE EDITOR

The conformational shifts of the voltage sensing domains between Na_vRh and Na_vAb

Cell Research (2013) **23**:444-447. doi:10.1038/cr.2012.158; published online 13 November 2012

Dear Editor,

Voltage sensing domains (VSDs), also known as voltage sensors, are electromechanical coupling devices that convert the membrane potential changes to the activation of voltage-gated ion channels. VSDs comprise four transmembrane segments (S1-S4), among which the S4 segment contains repeating positively charged residues (gating charges) that are exposed from the intracellular side to the extracellular milieus in response to membrane depolarization. A charge transfer center (CTC) that consists of two negatively charged residues and a conserved aromatic residue on the S2 segment was identified [1]. The two negatively charged amino acids, namely An1 and An2, may sequentially interact with the gating charges to lower the energy barrier during voltage-dependent charge transfer (Supplementary information, Figure S1) [2].

The recently reported crystal structures of two bacterial orthologues of the voltage-gated sodium (Na_v) channels, Na_vAb and Na_vRh, exhibited distinct conformations of the VSDs [3, 4]. In Na_vRh structure, all the four Arg residues, R1 through R4, point to the extracellular side across the occluding Phe residue on the S2 segment. In Na_vAb, however, R1-R3 are "up" while R4 remains on the intracellular side. That is, for each VSD, Na_vRh appears to transfer one more charge to the extracellular side [4]. When the two structures are compared with the pore domains as the reference, the four VSDs of Na_vRh must rotate around the pore domain by approximately 30° to reach the position of VSDs in Na_vAb (Figure 1A , Supplementary information, Movie S1) [4]. Here we present a systematic analysis of the conformational changes between Na_vRh and Na_vAb, focusing on their VSDs. As will be discussed, a combination of lateral rotation of VSDs around the pore domain and intra-domain rearrangements of VSD segments leads to the charge transfer of R4 across the occluding Phe (Supplementary information, Movie S1). A number of morphs were generated to facilitate visualization of the structural changes between Na_vRh and Na_vAb (Supplementary information, Data S1).

During the lateral rotation of the VSDs from Na_vRh to Na_vAb, the C-terminal fragment of S2 and the N-terminal helix of S3 appear to displace almost as one modular unit (Supplementary information, Figure S2 and Movie S2). Nevertheless, when a morph was generated to examine the conformational changes of the VSD segments relative to the CTC on the S2 segment, it appears that the S3 segment undergoes subtle but discernible rotation around its helical axis (Supplementary information, Movie S3). In contrast, the S1 and S4 segments undergo marked displacement relative to the CTC. The unwound C-terminal fragment of the S3 segment and the flexible S3-S4 linker allow major conformational shift of S4 segment relative to S2 and S3 segments. Similarly, the long S1-S2 linker supports the relative motion between S1 and S2 segments (Supplementary information, Movie S3). Interestingly, S4 undergoes self-rotation in addition to the 3_{10} to α helical transition when the structures are superimposed relative to the S1 segment; otherwise S1 and S4 segments would appear to stand approximately parallel to each other in both structures and move like a single module (Supplementary information, Movie S4).

Next we examined the shifts of VSD segments relative to the S4-5 linker helices in Na_vRh and Na_vAb (Supplementary information, Figure S3). Among the four VSD segments S4 exhibits the smallest displacement relative to the S4-5 helix, likely due to the constraint from the short linker that demarcates the S4-5 helix and the S4 segment (Supplementary information, Figure S3A). The S1 and S3 segments appear to undergo swing motions pivoting around the extracellular end of S1 and the intracellular end of S3, respectively (Supplementary information, Figure S3B). Interestingly, despite the R4 transfer relative to the CTC, the gating charges remain at similar altitudes within the lipid bilayer relative to the S4-5 helices in the two structures (Supplementary information, Figure S3C). In contrast, the S2 segment of Na_vRh, on which the CTC is located, is displaced by approximately one helical turn toward the intracellular side relative to the S4-5 helix compared to that in Na_vAb. Consequently,

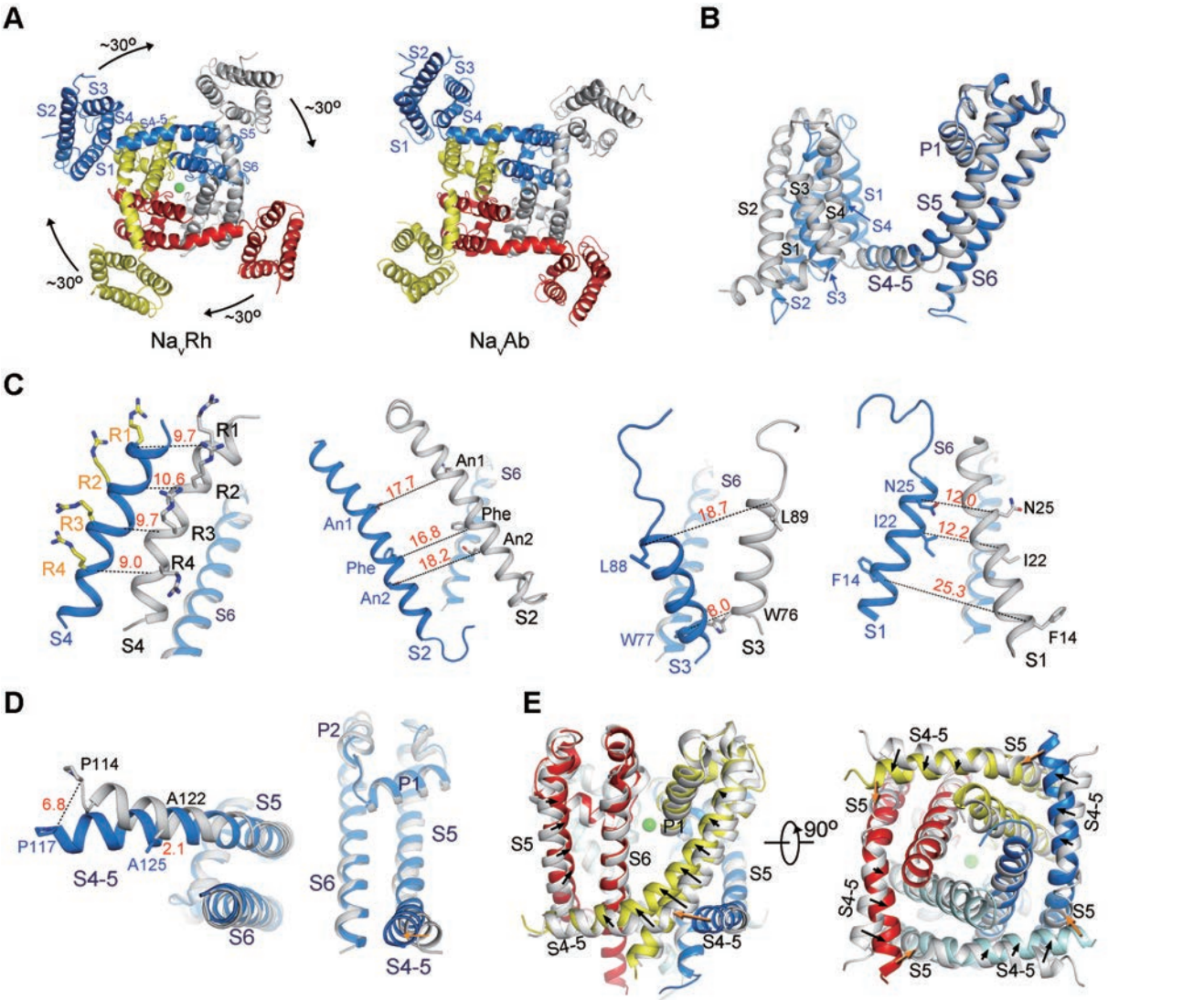

Figure 1 The conformational shifts between Na_vRh and Na_vAb. **(A)** Lateral rotation of the VSDs between Na_vRh and Na_vAb when the pore domains are superimposed. A cytoplasmic view is shown. Please refer to Supplementary information, Movie S1 for a morph of the overall conformational changes between Na_vRh and Na_vAb. **(B)** Structural changes between individual protomers when the structures of the tetrameric Na_vRh and Na_vAb are superimposed relative to the pore domains. Na_vRh and Na_vAb are colored blue and grey, respectively. **(C)** Dissection of the conformational shifts of the VSD segments relative to the pore domain. The S6 segments are shown in each panel as the reference to indicate the orientation of the structures. **(D)** The conformational shifts of the S4-5 helix as well as the S5 segment relative to the pore. A cytoplasmic view and a side view are shown. **(E)** The S4-5 helices and S5 segments are shifted (indicated by the black arrows) between Na_vRh and Na_vAb. The pore domain of Na_vRh is colored the same as in **(C)**, and that of Na_vAb is colored silver. The orange arrows indicate the potential pushing force exerted from the adjacent protomer during the conformational changes of its VSD.

R4 in Na_vRh is located on the extracellular side of the occluding Phe, while R4 in Na_vAb remains on the intracellular side (Supplementary information, Figure S3D). In another word, inward motion of S2 results in the R4 transfer to the extracellular environment when the S4-5 linker helices are superimposed.

Notably, the S4-5 helix and S5 segment also undergo considerable conformational changes relative to the pore domains of Na_vRh and Na_vAb. We then scrutinized conformational shifts of the VSD segments, the S4-5 helix, and the S5 segment when the pore domains are superimposed. The structural comparison of individual protomers from Na_vRh and Na_vAb is discussed below (Figure 1B).

R1-R4 appear to remain at similar heights within

membrane relative to the pore domain despite an almost horizontal translation of the S4 segment by about 9-10 Å (Figure 1C). The remarkable displacement of S2 segment relative to the pore domain is manifested by the 17.7, 16.8, and 18.2 Å shifts of the Cα atoms of An1, occluding Phe, and An2, respectively, through both horizontal and vertical translations between the two structures. Consequently, the S2 segment translocates towards the intracellular side by more than one helical turn in Na_vRh than in Na_vAb relative to the pore. The S1 and S3 segments exhibit translational shifts concordant with the overall VSD displacement relative to the pore in addition to their swing motions (Figure 1C).

The voltage-dependent shifts of VSDs leads to conformational changes of the pore domain. The S4-5 linker helix connects the VSD to the pore domain. Viewed from the cytoplasmic side, Pro117 in Na_vRh, which demarcates the VSD and the S4-5 helix, is tugged toward the center of the pore by about 6.8 Å from the corresponding Pro114 in Na_vAb (Figure 1D). Consistently, VSDs exhibit distinct interactions with the pore domains in Na_vRh and Na_vAb, although hydrophobic residues of S4 segment interact with S5 segment from the adjacent protomer in both structures. In Na_vRh, residues on the S1 and S4 segments contact the S5 segment of the adjacent protomer through extensive van der Waals interactions. By contrast, in Na_vAb, S1 barely touches S5 other than the contact at the extracellular tip (Supplementary information, Figure S4 and Movie S5).

If VSDs of Na_vAb were to adopt the same conformation as those of Na_vRh, the S4 segment would clash into the S5 segment of the adjacent protomer (Supplementary information, Figure S5A). In fact, the S5 helices appear to be pushed toward the selectivity filter in Na_vRh compared to those in Na_vAb (Figure 1E). Notably, the distances between the N-terminal tip of the S4-5 helix and the base of the S5 segment in the adjacent protomer remain nearly unchanged despite the extensive structural shifts between Na_vAb and Na_vRh (Supplementary information, Figure S5B and Movie S6), indicating a coupled motion between the adjacent protomers. This structural observation may provide an appealing explanation for the concerted transition of the four subunits in response to voltage [5, 6]. On the other hand, the conformational changes of the VSDs and the S4-5 linker helices may also contribute to the motion of S5 in the same protomer (Figure 1E). Therefore, the coupling between the conformational changes of the VSDs and the pore domain appears to be a very intricate process that awaits further dissection.

To summarize the observed conformational shifts of VSDs between Na_vRh and Na_vAb: VSDs as a structural domain undergo approximately 30° lateral rotation around the pore domain (Supplementary information, Movies S1 and S7). The VSD segments and the S4-5 helix exhibit discordant conformational changes. S3 shows limited rotation relative to S2, so does S4 to S1 (Supplementary information, Movies S2-S4). The module formed by S1 and S4 undergoes pronounced movement relative to that by S2 and S3 (Supplementary information, Movies S3, S4). During the outward R4 transfer across the occluding Phe from Na_vAb to Na_vRh, R1-R4 on the S4 segment appear to be positioned at almost identical altitudes within the lipid bilayer, while both vertical and horizontal shifts of the S2 segment result in the R4 transfer across the occluding Phe (Supplementary information, Movie S7). This structural analysis appears to be supported by the experimental observation that the S2 segments undergo conformational changes preceding S4 in the *shaker* K^+ channel [7]. Notably, the lipid composition must be important to the electrophysiological property of voltage-gated channels as the VSDs undergo lateral rotation within the membrane bilayer, an analysis consistent with numerous lines of experimental evidence [8, 9].

The structure-based comparison of VSDs between Na_vRh and Na_vAb reported here suggests an extra possibility to achieve charge transfer in addition, but not exclusive, to the existing models [2]. Notably, when Na_vRh-VSD is compared to KvAP-VSD [10], the structural differences are obvious (Supplementary information, Figure S6). In Na_vRh, the S1-S2 and S3-S4 linkers are long and flexible, which provides the molecular basis to allow the shifts between S1 and S2, S3 and S4, respectively. In contrast, the S3 helix of KvAP is broken in the middle, whereas the linkers between S1-S2 and S3-S4 are short and tight. Therefore, KvAP-VSD may not be able to undergo similar structural changes illustrated for Na_vRh and Na_vAb, because the short linkers may restrain the relative motions between the corresponding segments. Rather, the unwound region in the middle of S3 may provide the molecular basis for a paddle motion of the voltage sensor [11].

It is noteworthy that one caveat limits further interpretation of the structural observations. What are the states that the structures of Na_vRh and Na_vAb each represent? Na_vRh was suggested to be captured in an inactivated conformation [4], whereas Na_vAb was reported to reflect a "pre-open" conformation [3]. Two extra crystal structures of Na_vAb were published to be in inactivated states [12]. Nevertheless, the structural comparisons discussed here can be applied to the new Na_vAb structures, because the latter two can be superimposed to the first Na_vAb structure with rmsd values of 1.6 and 1.2 Å over 874 and

852 Cα atoms, respectively. Then what physiological process does the R4 transfer between Na_vRh and Na_vAb indicate during voltage sensing? The answer remains elusive. Further experimental analysis, molecular dynamics simulations, and more structural evidence are required to understand the physiological relevance as well as the general implications of the structural changes between Na_vRh and Na_vAb. Nevertheless, the structural comparison illustrated here provides a new possibility to achieve charge transfer for the VSDs of voltage-gated ion channels.

Acknowledgments

This work was supported by the Ministry of Science and Technology (2009CB918802 and 2011CB910501), and the National Natural Science Foundation of China (91017011 and 31070644), and funds from Tsinghua University.

Xu Zhang[1], Nieng Yan[1]

[1]*State Key Laboratory of Bio-membrane and Membrane Biotechnology, Center for Structural Biology, School of Life Sciences and School of Medicine, Tsinghua-Peking Center for Life Sciences, Tsinghua University, Beijing 100084, China*
Correspondence: Nieng Yan
Tel: +86-10-62771298; Fax: +86-10-62792736
E-mail: nyan@tsinghua.edu.cn

References

1 Tao X, Lee A, Limapichat W, *et al*. *Science* 2010; **328**: 67-73.
2 Catterall WA. *Neuron* 2010; **67**: 915-928.
3 Payandeh J, Scheuer T, Zheng N, *et al*. *Nature* 2011; **475**: 353-358.
4 Zhang X, Ren W, DeCaen P, *et al*. *Nature* 2012; **486**: 130-134.
5 Zagotta WN, Hoshi T, Aldrich RW. *J Gen Physiol* 1994; **103**: 321-362.
6 Kuzmenkin A, Bezanilla F, Correa AM. *J Gen Physiol* 2004; **124**: 349-356.
7 Cha A, Bezanilla F. *Neuron* 1997; **19**: 1127-1140.
8 Schmidt D, Cross SR, MacKinnon R. *J Mol Biol* 2009; **390**: 902-912.
9 Schmidt D, Jiang QX, MacKinnon R. *Nature* 2006; **444**: 775-779.
10 Butterwick JA, MacKinnon R. *J Mol Biol* 2010; **403**: 591-606.
11 Ruta V, Chen J, MacKinnon R. *Cell* 2005; **123**: 463-475.
12 Payandeh J, Gamal El-Din TM, Scheuer T, *et al*. *Nature* 2012; **486**: 135-139.

(**Supplementary information** is linked to the online version of the paper on the *Cell Research* website.)